Uncertainties related to strain measurements in piles

by

Himani Arya

Student number:	5161614
Project duration:	October 15, 2020 – May 25, 2022
Thesis committee:	Prof. K. Gavin, TU Delft, supervisor
	Kevin Duffy, TU Delft

An electronic version of this thesis is available at
http://repository.tudelft.nl/.

Preface

This thesis report contribute to the intend of research work from the student of Delft University of Technology. It aims to analyse difference between strains data measured by fiber optics, strain gauges, centrifuge and theoretical stress-strain relation while loading a model pile and can present for the further research on the specifications of the datalogger and reasons behind the discrepancies in the data obtained by different techniques for future use. This work would not have been possible without P.H.D candidate Kevin Duffy and Lab technicians.

Readers interested in obtaining more insight about potential reasons behind inconsistencies in strain measuring theories and devices can touch on to the content of this additional thesis report.

Himani Arya
Delft,May 2022

1

Abstract

In recent years, distributed fiber optic sensing (DFOS) technology has been widely used in monitoring the strains developed in the structures.

The main focus of this report is to identify strains distribution while hammering/ jacking pile and analyzing the uncertainties between the theoretical, measured strain through datalogger in concrete and steel piles. This assessment is done to gain confidence over the feasibility of using DFOS technology. Fiber optic cables are embedded all along the length of the concrete and steel piles with ends connected to the datalogger. To confirm the accuracy of the datalogger, other strain measuring devices like load cell and strain gauges are also glued to the piles.

For both the piles load with in the yield limit is applied and strains are measured. fTb 2505 datalogger posses high accuracy with lower spatial resolution where as Luna Odisi datalogger has high spatial resolution and less accuracy which can be directly reflected through the strains obtained from both datalogger. Results obtained from steel pile reflects that strains obtained from Luna Odisi datalogger and load cell matches with in the accuracy and with no slippage . But for concrete piles fTb 2505 datalogger shows more fluctuating strains as compared to the strain gauges with uncertainties included in both the devices.

Contents

List of Figures

List of Tables

2

Introduction

In modern times, most cities are densely populated accompanied by a shortage of land for proper foundations of houses, skyscrapers. Foundations help in distributing the load of the structure to the soil layer and can be either shallow or deep. Often deep foundations are used as a support for wind turbines, car parking, bridges, dams, etc, and transfer the load to a layer with high bearing capacity. These foundations can be in the form of piles that can either be bored or driven depending on the soil type and the location. They can also be hollow or solid, precast or steel pipes depending on the requirements.

Driving piles through hammering can cause the generation of locked-in stresses (residual loads), bending, and strains. Residual loads affect the bearing capacity of the pile. To understand what happens while hammering a pile, fiber optic cables are embedded throughout the length of the pile. These cables can measure strains and temperature changes in piles with the help of a data logger that works on new BOFDA technology.

The objective of this project is to design a 1G model of piles and study difference in strain values measured theoretically, through datalogger and strain gauges generated while loading.

The first chapters of this report illustrate the general background knowledge required to understand pile, fiber optics working, the data logger used to interpret data and the effects of hammering on strains. The second chapter will communicate the methodology used to design, cast, and strain calculations. The third chapter will accompany to look into the distribution of strains in concrete and steel piles and the difference between the theoretical and practical stress-strain relationships. In the end discussions and conclusions will be made regarding the accuracy of the data logger, residual loads, effects of coating.

3

Literature Review

3.1. Piles

Figure 3.1: Precasted pile

The primary purpose of the pile foundation is to transfer the load of the structure through a layer of poor bearing capacity to the one of adequate bearing capacity. Pile lengths can vary from 5m to 40m and can differ in size depending on the strength required to support the structure above. They can be made out of concrete with a reinforcement cage inside or hollow steel pipes. According to the surrounding, piles can either be driven or bored. Driving a pile seems more conventional than boring off-shores since the precision required for boring is hard to attain. The hammering, jacking, or vibratory method can be helpful for installation (Figure 3.1). Each

technique have their advantages and disadvantages, for example, vibrations create abundant damages like cracks and settlements in the surroundings, and hammering piles produces noise [9]. Hammering applied to the pile head leads to the movement of the pile into the soil, causing strain and residual loads build up.

Increase in the size of the piles, different loading techniques and varying soil conditions have resulted in uncertainties over existing design methodology due to lack of past experiences and field data [24],[21]. And modeling a pile can provide an insight into what happens during installation in the pile with the help of fiber optic cables embedded into the pile.

3.2. Optical Fiber sensors

Monitoring the health of the structures (offshore piles, bridges) in terms of cracking and corrosion has become an important issue worldwide for maintenance and workability [13]. Deformation in the pile caused in response to the hammering can be monitored with various monitoring techniques. Conventional instruments used for monitoring work include displacement transducers to measure vertical deflections at the top of the pile, load cells for applied load and embedded vibrating strain gauges, extensometers for relative displacement measurement within the piles. However, distributed fiber optic sensing (DFOS) based on Brillouin scattering has been a great alternative for strain over point sensors, as they provide a high spatial density of data throughout the length of the pile[14],[18]. DFOS datalogger is connected to fiber optic cables for evaluating strains. These cables are lightweight, cost-efficient, and are reliable.

Temperature measurement: The cable used for measuring temperature change has two protective layers, an outermost protective layer and another layer of a tube made out of either steel or polymer. Figure 3.2 illustrates the inner structure of the fiber. Optical fiber/glass fiber with free length embedded inside two covering layers and surrounding the fiber is the fluid that acts as a defense. Since the fiber is not bonded with any protected layer, it does not get subjected to any mechanical strains while stresses are applied.

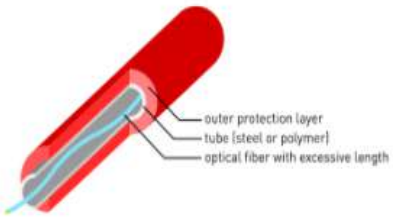

Figure 3.2: Temperature measurement fiber[6]

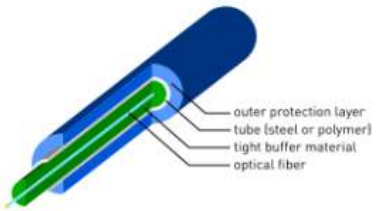

Figure 3.3: Strain measurement fiber [6]

Strain measurement:

The basic structure of the fibers consists of 3 components inner core, cladding, and outermost coating. The core is positioned at the center for sensing strains and is tightened (tensioned) for the better transfer of the mechanical stress Figure 3.3. It is a glass fiber that is fragile and could be get crippled easily with sharp curves and bends and to protect it, a coating is applied. This coating can cancel out some forces and also helps in the transfer of loads. The coating can be made out of either nylon, polyimide, or other polymers. Fibers with nylon coating tend to be cheap as compared to polyimide ones. Nylon coating is applied to the exterior of cladding with the jacking technique. This method makes the coating not get chemically cured onto the core. As a result, the coating is not bonded with the core and causes inaccurate strains while transferring loads since nylon would slip over coating [8]. While polyimide coating is chemically bonded with the core which prevents the problem of slippage. The important note here is that both the fibers can detect cracks but errors in nylon coating are much higher than in polyimide ones [8].

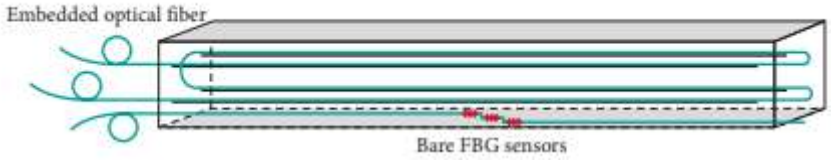

Figure 3.4: Fibre sensors are attached to reinforcement[28]

Depending on the requirement, the cables can be attached to the pile, and figure 3.4 shows one of the arrangements. Fiber optic cable length needs to be long enough that it can be wrapped around in a close loop and some extra length to be attached to the monitoring datalogger.

In long piles, cables are either be laid down along the reinforcement cages in pre-casted ones or glued with epoxy or superglue onto the surface of steel piles. Epoxy is a compound made from two parts a resin and a hardener that is needed to be combined. There is a specific time window, based on the package instructions, in which the glue is applied before it hardens. And super glue or cyanoacrylate is a single component that hardens rapidly with exposure to moisture in the air. Gluing a cable with epoxy does not hamper the measurements and load transfer as no slip between the fiber and pile surface occurs [3],[10].

Optical fiber needs to be connected to a readout datalogger to capture the changes in strains and temperature within the pile while loading.

3.3. The fTB 2505 series and Luna odisi 23.5 Hz HD Datalogger

A data logger is output equipment that is required for monitoring the distributed fiber-optic readings and providing strain and temperature values along the length. The fTB 2505 series Datalogger adopts the principle of quasi-continuous measure-

ment and works on the phenomenon of Brillouin light scattering. This technology is called Brillouin optical frequency domain analysis (BOFDA).

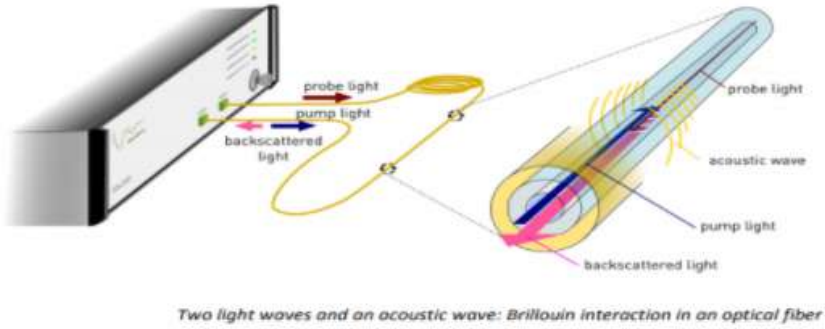

Figure 3.5: Working of the ftb 2005 data logger sensor [6]

Working :A light wave of a certain frequency is injected to both the ends of the optical fiber from the data logger figure 3.5. And when these waves meet each other in the cable they develop acoustic waves because of the increase in the intensity of the light. This acoustic wave develops disturbances in the pathway of the light [6] and makes the fiber shiver. These disturbances, when propagated forward, lead to backscattering of the light. Now this backscattered light meets the incoming waves and forms more acoustic waves. This process keeps on going as a self-amplifying effect. To limit this process offset is set with the speed of sound in the fibers. The maximum backscattering is captured by the instrument with time and sonic speed is calculated then of the fiber which is directly proportional to strains and temperature [13] for time. The performance, features, and technical data of the data logger plays a crucial role to understand the device 3.1

1. Spatial Resolution: refers to the optical pulse length that inspects brillouin interaction along the cable length. Shorter the length more precise the data will be obtained. For long lengths high spatial resolution is desired for faster measurements.

2. Spatial accuracy: distance between two measurement points in the measurement curve of the strain/ temperature profile. This provide more details related to exact position and shape of strains along the fiber length.

3. Acquisition time: time taken to attain the precise value.

4. Accuracy: deviation between measured value and true value.

Loss of light is the issue while using BOFDA technology. As soon as probe light is ejected out from the datalogger, with each connection, bends, noises, etc, some

No.	Feature	fTB2505 Value	Luna odisi
1	Spatial Resolution	0.2m for 1km	0.65mm
2	Accuracy(Strain)	$< 2\mu\epsilon$	$< 20\mu\epsilon$
3	Accuracy(Temperature)	$<0.1°C$	$<0.1°C$

Table 3.1: Performance,features and technical data of ftb 2005 ,Luna odisi data logger [15],[6]

of the light frequency is lost [17]. These optical losses are limited till 20dB [6]. But high losses can lead to errors in the strains and temperature accuracy values all along with the FO.

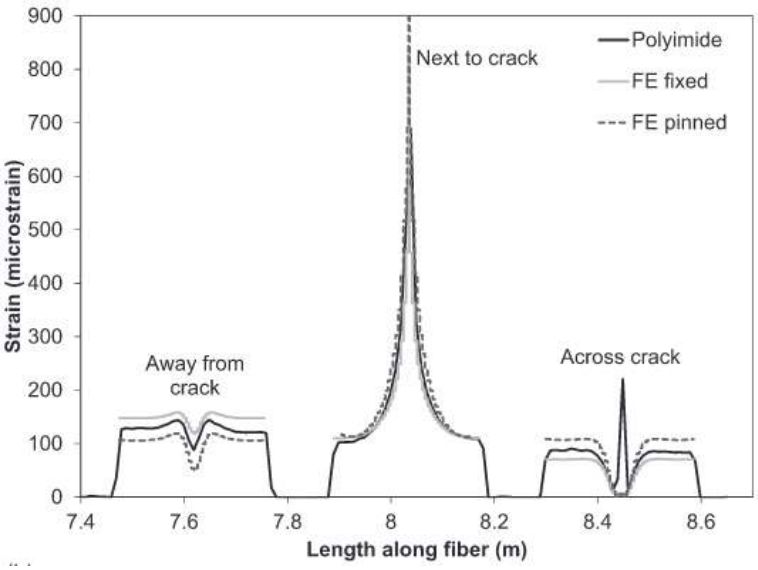

Figure 3.6: Rise of strain near crack [8]

BOFDA technology can measure both strains and temperature change throughout the length of the cable [12], [4]. But identifying the exact location of the cracks, localized strain is still a challenge of the technology with low-resolution [28]. Crackings on the concrete beam also affect the strain transmission of the internal optical fiber. As Location of the vertical cracks leads to stress concentration in the optical fibers [29] and [25]. This can cause the strain curve to rise suddenly near the crack Figure 3.6. And if the horizontal cracks connect optical fiber may separate from the interface of the concrete. While the fiber clamped outside the pile remains unaffected by the crack since deployment allows the fiber to leap over the crack. Comparing the strains from FO and strain gauges is a hard task location does not match, there can be crack under the strain gauge or bonding mistake with concrete [3] leading to inappropriate strain values.

3.4. Theoretical stress- strain relationship

From the fiber optic cables, the strains are calculated throughout the length of the pile. But theoretical stress-strain distribution both steel and concrete piles is different.

3.4.1. Concrete:

There is a non-linear relationship that is observed in the stress-strain curve of concrete with ultimate state analysis under combined flexure and axial load of high-strength concrete. Figure 3.7 , shows the stress-strain relationship of the concrete ([27].

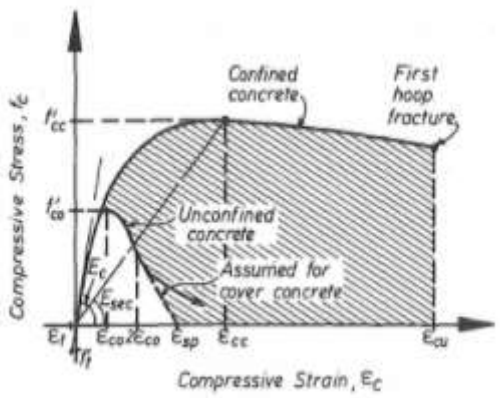

Figure 3.7: Stress-Strain Relation of Concrete ([27])

f'_{cc} is compressive strength (peak stress) confined concrete,f'_{co} is compressive strength of unconfined concrete,ϵ'_{cc} is defined as strain at maximum confined concrete, and $\epsilon'_{uc}$is strain at maximum unconfined concrete.

The concrete block with transverse reinforcements is called confined concrete whereas one without any reinforcement is called unconfined concrete. Since model pile will posses no soil support, it is probably be going to behave like unconfined concrete or not going to completely replicate the stress-strain graph.

Brittle, elastic material like concrete tends to generate cracks parallel to the maximum compressive stress. The cracks in the concrete occur due to micro cracking which are the internal cracks along the interface of the paste and aggregate called bond cracks and mortar cracks.

Stages of cracking in concrete [16]

1. Concrete shrinks while hydration and tends to develop no load bond cracks. Stress strain remains linear upto 30% of the compressive strength. We can define this linear behaviour as elastic behaviour.

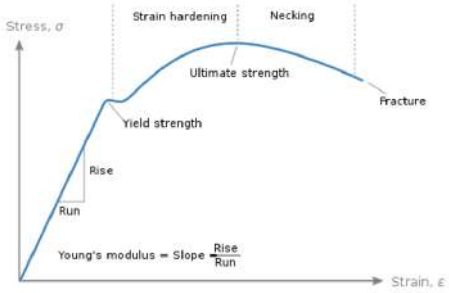

Figure 3.8: Stress strain of steel [30]

2. At 30-40% of compressive strength leads to development of new bond cracks. However additional load will be redistributed to the unbroken interfaces and mortar.

3. Localized mortar cracks develop between bond cracks at 50-60% of compressive strength. At this stage cracks develop parallel to compressive loads and due to transverse strains.

4. 78-80% of ultimate load, continuous patterns of microcracks begin to form. More nonlinear stress strain graph is visible

3.4.2. Steel

The theoretical stress-strain relationship for steel S255 (Figure 3.8)gives an idea about the behavior of steel when a compressive load is applied. The theory provides an intuition of elastic and plastic strains. Loading steel beyond the yield limit permanently can cause deformation in the material. Stress-strain remains linear up to 20% of the proof strength (85-90 % of yield strength)([11]). The ultimate strength of the steel S255 with a thickness of 3mm would be around 350-400 MPa. However, no specific values differentiating between yield and ultimate strength can be obtained through this theory. In real life, steel might deviate from the graphical illustration provided [30].

Knowing the young's modulus of material and the dimensions, one can directly calculate the residual loads induced in the piles.

$$Q = EA\epsilon \tag{3.1}$$

Q = residual loads developed on piles
E =Young's modulus of pile
A = Area of the pile
ϵ= strains measured in the pile

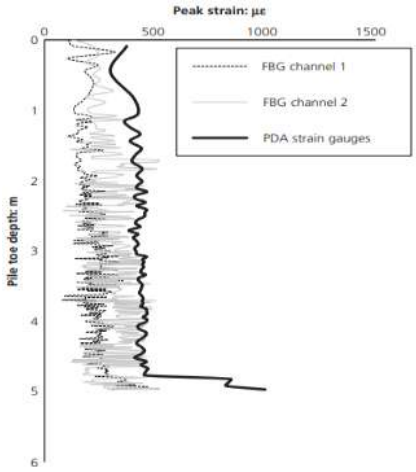

Figure 3.9: Strains measured in PDA and FBG [5]

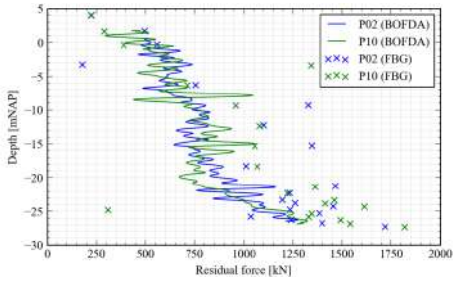

Figure 3.10: BOFDA, FBG cables in same pile

3.5. Effects of hammering

After the hammer blow, the pile tends to move downwards but pile-soil friction tends to resist by acting upwards (rebounding). During rebound, the pile pushes itself upwards and decompresses elastically. Equilibrium is attained after enough friction stresses (upper half) have reversed keeping the bottom pile stressed against the soil. The process of loading and unloading can cause the generation of residual load into the pile([1], [2]). Residual load or locked-in stresses distribution also depends on the layering of soil strata and load intensity. They tend to increase when the relative stiffness of the pile decreases and maximum are expected at the pile toe ([22]). A general theory about the development of the residual loads in piles, explains that pile has a neutral plane, positive skin friction (lower part), and negative skin friction(upper part) [20]. It is supposed that above the neutral plane, the residual loads keep on increasing with depth until it reaches the neutral axis and, later in the positive skin friction the residual loads keep on decreasing. This theory is a hypothesis because residual load distribution varies in different cases ([22], [20],[23]). However, it is important to take account of residual loads for the interpretation of bearing capacity and shaft capacity. Residual loads are also generated during the casting of the piles, the swelling period, and build-up due to driving the pile [?].

Hammering also leads to bending which mainly occurs at near pile head due to poor confinement under axial loading and axial shortening of the pile [12]. It depends on eccentricity during axial loading and soil strata in which pile is pushed [7]. Another effect of hammering is the displacement of the sensors on the head of the pile with respect to the toe of the pile [5] Figure 3.9.

While installing 3 concrete piles, embedded with FBG, temperature cable, and BOFDA fibers at a test site in Amaliahaven, Maasvlakte 2, Port of Rotterdam,

an observation was made regarding the residual forces obtained by the FBG and BOFDA. Both measurements do not replicate each other Figure 3.10. A huge gap between the values can be seen from 10-15m of depth. To have a closer inspection behind the reasoning of such discrepancies (damage to the cable, transfer of forces to the fibers, etc), this additional thesis had been proposed.

1. Dissimilarity between the theoretical and measured strain obtained from datalogger while loading a pile?
2. Identifying the noticeable effect in terms strain levels by using different type of glues and optical fiber with and without coating?
3. Is the accuracy of data logger on specification document verifiable while comparing it with strain levels in gauges or centrifuge ?

4

Methodology

This report aims to replicate the actual pile in a scaled model, then look for the strains throughout the pile length. Both precast concrete (with reinforcement) and hollow steel pile have been used for the study.

4.1. Concrete pile

Designing a model pile with the fiber optic cables embedded inside is done prior to any step. While planning out pile it is necessary to start with the forces/load that will be applied to the pile head. This will further help in deciding the size and the ultimate load capacity of the pile.

4.1.1. Pile design

Calculation of forces:

A hammer will be released from a certain height, gravity will lead to transfer of the Potential Energy into K.E. With work energy equation,

$$Impactforce * distancetravelled = K.E \tag{4.1}$$

and in this case Kinetic Energy= Potential Energy,
hence

$$Impactforce = m.g.h/d \tag{4.2}$$

Considering the hammer weight m=25kg and h=1.5m keeping d as minimum=0.001m will give maximum force applied on the hammerImpact force= 367.5 kN. If height is decreased to 1 m then F=245.250kN. m=mass Kg
g=9.8 m/s2
h= falling height m
d= displacement m

Design Load on the pile:

$$P_u = 0.4.f_{ck}.A_c + 0.67.f_y.A_{sc} \tag{4.3}$$

Where,
P_u = Ultimate Load of the Column in N
f_{ck}= Yield Strength of Concrete in $= (20 * 10^6 N/m2)$
f_y = Yield Strength Of Steel in= $(220 * 10^6 N/m2)$
A_{sc}= Area of Steel (Cross-Sectional Area) in Column in.$0002m^2$
a_c = Area of Concrete (Cross-Sectional Area) of Column =0.03m2

Considering diameter of steel bar 16mm and 48mm length,

$$P_u = 0.4.f_{ck}.A_c + 0.67.f_y.A_{sc} = 240 + 29.621 = 269.641kN \tag{4.4}$$

Design load on a pile would be 270kN and force applied on the pile by dropping a hammer of 25kg from 1m height would be 245kN. Hence applied load would be lesser than designed load. Accordingly, the dimensions of the pile can be 20*15*50cm and the reinforcement can be 48cm height and 16mm diameter. Further design calculations for the pile are attached in the appendix of the report.

4.1.2. Modeling a pile

To recreate a model pile, length of a pile needs to be scaled down by the factor N.

$$L_{Model} = \frac{L_{Prototype}}{N} \tag{4.5}$$

Scaling of the aggregate of the pile: Cross-sectional area of the prototype pile is 350mm but an area of the model pile is 300mm. The size of concrete is 10mm in diameter. So when load will be applied to the pile, the contribution of each particle of concrete will be more than prototype pile. This might hamper the distribution of load into the pile.

4.1.3. Instrumentation Description

In the preceding section dimension of the pile =20*15*50cm is decided. Now a wooden mould with considerable dimensions is constructed with hard plywood, which is drilled and screwed together. This detachable mould can be easily removed without causing any additional cracks and damage to the pile after curing.

Extra holes of a diameter greater than the wire are also drilled on the opposite sides of the wooden mould. These holes work as the inlet and outlet for the optic fibers and are surrounded by foam and glass tubes to secure the breakage of fibers inside through steep curves. Planning is done for the arrangement of the optical fiber inside the mould. In the middle of the mould, a reinforcement is hung of 45cm, 90mm diameter carefully with the help of transparent strings tightly hung by board pins. These strings are strong enough to hold the reinforcement in the mould. To fix the fibers glue had been applied to the holes. Length of the fiber optic cable inside the pile is 10m and in total fiber used is 50m.

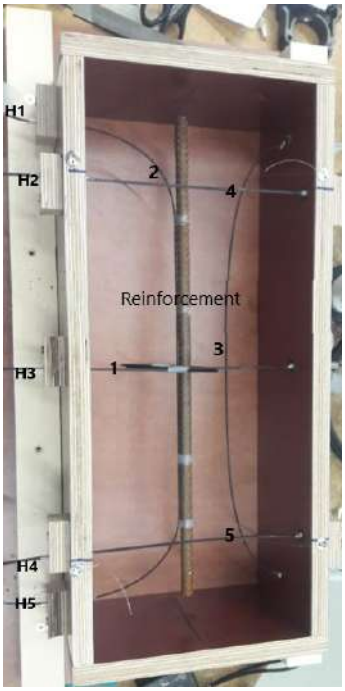

Figure 4.1: Wooden mould with reinforcement and optic fiber

There are 5 ways in which the fiber is arranged in the wooden mould 4.1.

1. Starting from the middle of the mould, the fiber is laid on the rod in form of the loop and passing the wire through it at the center. In order restrict its movement wire has been taped tighter in the middle.

2. Addition 1.5m of wire had been left free and then wire is attached to the reinforcement with the help of tape.

3. An extra fiber is attached at parallel but at some distance from the rod. After pile getting cured this wire will be directly attached to the concrete.

4. 2 fibers are laid down at the top and bottom of the mould perpendicular to the reinforcement at the distance of 12cm from edges.

After curing the concrete pile for 28 days, the wooden mould was detached. With the visual inspection, cracks on the surface can be recognized easily in figure 4.2 . These cracks can get wider when heavy load is applied and can lead to the failure. Traditional strain gauges are fixed in the middle of the pile on the opposite sides(fig:4.3). These strain gauges are stick to the pile surface with the help of glue and a foil. Certain uncertainties can occur while working with readings from the strain gauges[19], [26].

No.	Type	Length of fiber (outside+inside) pile
1	Loop	1.5m+0.75m
2	Along reinforcement	1.5m+0.5m
3	Into concrete	1.5m+0.5m
4	Perpendicular top	1.5m+0.20m
5	Perpendicular bottom	1.5m+0.20mm

Table 4.1: Fiber cable embedded length inside the pile

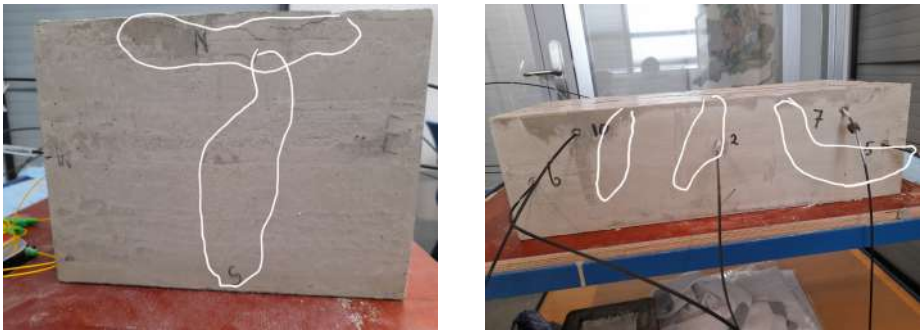

Figure 4.2: Cracks developed after curing

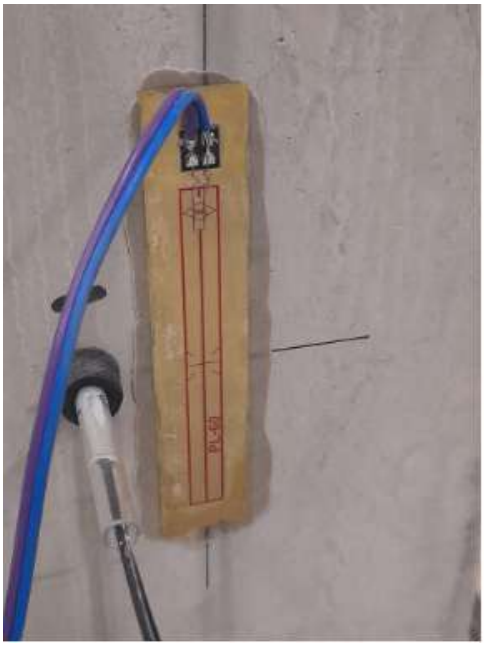

Figure 4.3: Strain gauge

4.1.4. Data analysis

Initially static loading is applied on the pile top by keeping direct weights of $5kg$ one over other (4.4). Simultaneously, strains are reproduced in the fTB 2505 series data logger and strain gauge corresponding to time to capture the effects after loading. The end of fiber cables are connected to the datalogger to calculate the strains change. Pulse collected by the datalogger through Brillouin scattering in the fiber optic cable is analyzed through data points. At various data points, the fiber optics analyzer stores vectors of peak Brillouin frequency. These frequencies need to be assigned to different locations of the cables. Since it is hard to identify exact location of the fiber inside the cable, we pull the cable segment next to pile entrance to get the hint about locations. And as soon as the location of the data point is identified, strains can be measured. Every reading obtained from the data logger illustrates data between time, length and strains. Then time is indicating certain strains is chosen from datalogger readings and accordingly same time is choose to make comparison between strain gauge and datalogger.

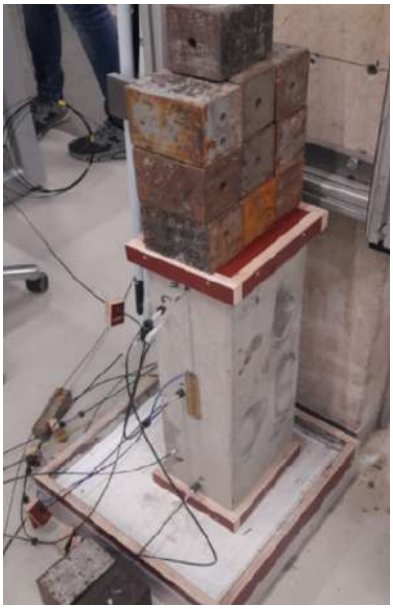

Figure 4.4: Static load on pile

4.2. Steel pile

A hollow square steel pile with the dimension of 45cm*30cm and thickness of 0.3cm is employed to apply loads. The grade of steel used is S255 which has the modulus of elasticity of 200000 MPa . Fujikura cable one with coating and the other without coating are glued next to each other on one side of the pile. This fiber cable has a coating of polyethylene. Figure 4.6 illustrates the layout of the cable (Fujikura) used.

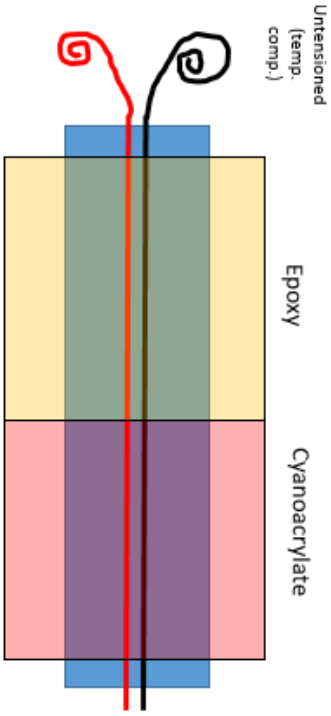

Figure 4.5: Illustration of glue applied on pile

Two different types of glue are used on the steel pile to stick the fibers on surface, upper half with epoxy, and the lower half with super glue Figure 4.5. Through jacking cyclic loads up to 30MPa are applied to the pile head causing, strains are measured with the datalogger. Instead of the fTb 2505 datalogger, a different Luna odisi 23.5 Hz HD datalogger with an accuracy of 20 micron strain has been used to study the effect of the coating on the fiber optic cables.

A quick test is done to investigate the accuracy of the another datalogger on the steel pile. This steel pile has a thickness of 0.3cm and 2 different fibers one with coating and one without coating glued next to each other on one side. The test is done within the yield limit of steel to understand the effect of coating and gluing on the optical fibers. An incremental cyclic loading has been applied to this pile

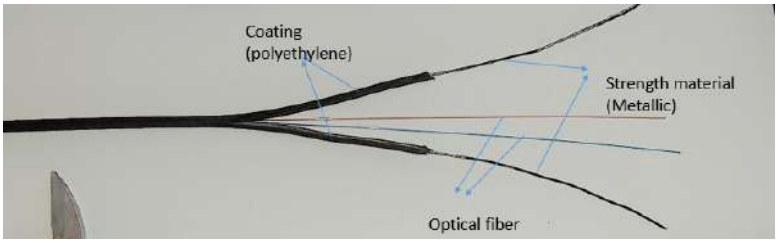

Figure 4.6: Layout of fiber cable (Fujikura)

through jacking in the centrifuge and a load cell was used to compare the results with a datalogger.

After completing the loading process on both the pile's data collected will be compiled and results are discussed.

5

Results and Discussions

5.1. Concrete pile

A concrete pile is precasted with reinforcement in the middle and optical fibers embedded at different locations. Datalogger ftb 2505 is used to investigate strains along the length of the pile while hammering the head. On opposite side of the pile (center), strain gauges are also glued. Table 5.1 shows list of load test done and than results in terms of micro strains obtained through gauges, theory and ftb2505 datalogger. This procedure of incremental static loading up to 50kg is implemented to look into difference in strains developed in reality, in theory and also accuracy of the datalogger specified.

Weight (kg)	Load (kPa)	Theoretical strain	Strain gauge	Datalogger(micro strain)
0	0	0	0,30274	-0,492
5	1,635	0,08175	1,22071	11,11
10	3,27	0,1635	3,47657	13,11
15	4,905	0,24525	3,65235	1,51
20	6,54	0,327	3,7793	-5,291
25	8,175	0,40875	4,70704	26,306
30	9,81	0,4905	4,83399	18,307
35	11,445	0,57225	7,05079	11,507
40	13,08	0,654	6,41602	30,706
50	16,35	0,8175	7,96875	46,51

Table 5.1: Test load applied and measured on concrete pile for static loading

Concrete pile has been embedded with the 5 arrangements of fiber optic cable and a reinforcement in the center. The place where fiber enters the pile can be identified by putting pressure on the fiber cable and looking for the responses in the datalogger but it becomes really hard to pick out the exact location of fiber inside the pile Figure 5.1. Some of the inputs received from these arrangements would be

discarded because they do not come in the range of desired length 20cm required to make a single calibration by the data logger ftb 2505. Since the pile is 50cm long, there are 2 arrangements of fiber that go through the length of the pile and satisfy the requirement. But the readings from the fiber attached to the reinforcement are only considered for the analysis due to neutral axis.

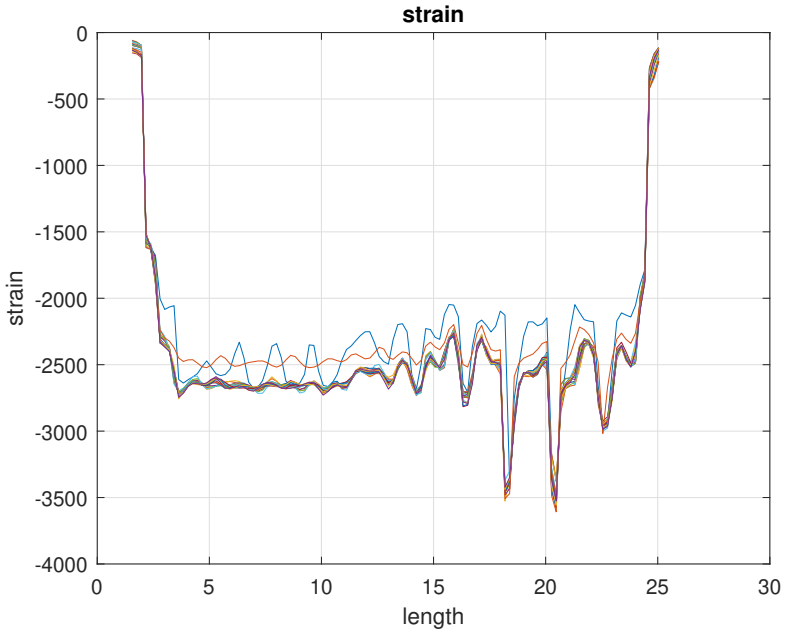

Figure 5.1: Strain reading through out the pile length in concrete pile

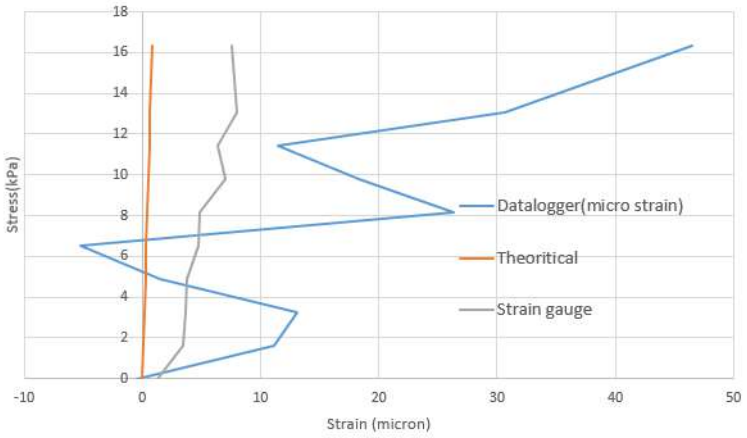

Figure 5.2: Strain measured theoretically, with datalogger and strain gauge for static loading

Figure 5.2 illustrates stress-strain relationship between concrete. The ultimate load for which the concrete pile has been designed is 270kN. But the maximum load applied on the pile top is less than 10% of the ultimate strength, hence only reversible elastic strains are observed throughout the pile length. A linear increase in strain values with the increase in stress till yield point (30% of ultimate load) is expected in the concrete piles through theoretical relation. Strain levels measured through the the strain gauges also show kind of linear relationship and they are attached to the center on opposite side. Although fiber optics is embedded through out the length but datalogger works takes up the highest strain obtained through out the 20cm length. Hence it is hard to point at the exact location where strains are measured by the devices.

Blow	Load(kpa)	Distance(m)	Data logger(micron)	Strain gauge(micron)
5	0,355776	0,1	20,793	6,15235
5	0,88944	0,25	43,192	11,15235
10	0,711552	0,1	73,189	14,62891
10	1,77888	0,25	30,793	16,15235

Table 5.2: Test load applied and measured on concrete pile for cyclic loading

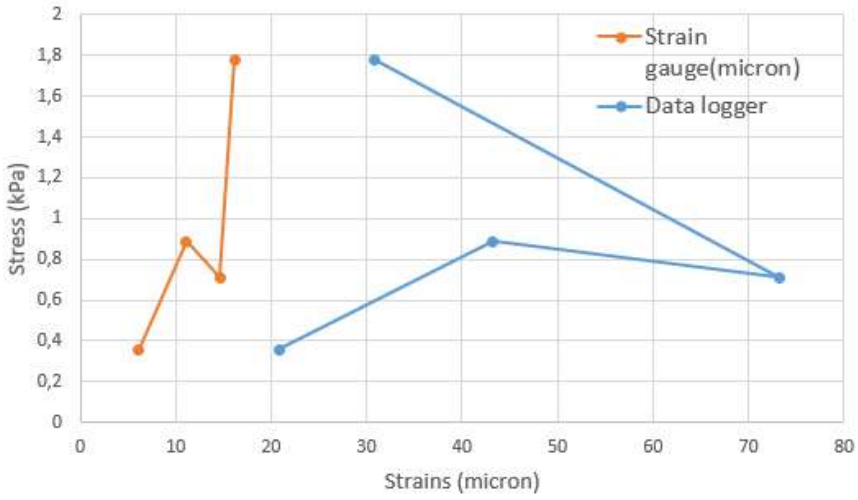

Figure 5.3: Strain measured with datalogger and strain gauge while hammering

Table 5.2 shows list of test done while dropping the hammer (2.175 kg) from certain height to replicate hammering effect. Results in terms of strain levels are illustrated in figure 5.3 and data obtained is been compared with strain gauge.

Comparing theoretical, gauge, and datalogger strain levels, it can be seen clearly that theoretical and gauge readings are relatively less varying then datalogger reading for static loading. Reasons for the uncertainties in strain value could be the

installation of the gauge, measuring procedure, signal processing, poor condition of the gauge and even shrinkage cracks. There were also some cracks can be observed from the outside look of the pile due to curing 4.2. It is also possible that datalogger is not meant to encapture such small strain levels and the specification mentioned in the datalogger ftb 2505 sheet about accuracy of 2 micron is not correct. Fluctuations in strain values obtained from datalogger can be the result of long length of fiber, poor handling during pile construction and noises.

5.2. Steel pile

	Strains (micron)			
Stress(Mpa)	Theoritical	Coating	Naked	Load cell
1,93	9,171075838	-18,11	-16,58	-94,4073
3,81	18,13051146	-12,52	-1,55	-51,3704
7,49	35,66137566	31,22	53	27,51852
18,67	88,88888889	272,24	295,94	265,1111
29,91	142,4338624	539	556	514,3333

Table 5.3: Load test applied and measured on steel pile

Figure 5.4 illustrates the stress-strain paths of the steel comprehended from Fiber optic cables (with coating, without coating), theoretically, and through a centrifuge. The strains obtained while jacking a pile in a centrifuge and strains monitored by both the fiber cables matches quite well. Since Luna odisi 23.5 Hz HD data logger is specified to provide accuracy up to 20 micro strains, that is why there is a deviation in the strains measured between the fibers. The maximum load applied on the pile was up to 30 Mpa. The ultimate strength of the steel S255 with a thickness of 3mm would be around 350-400 MPa. So it is postulated that the applied stress was around 10% of the ultimate stress. Hence, no signs of slipping are observed 5.4 while applying to load, since loads are within the yield curve and no plastic strains or deformation occurred during loading.

Two different types of glues epoxy and cyanoacrylate are applied to stick the cables on the steel surface. While analyzing data obtained from the BOFDA technology data logger, both the glue presented similar results. Fluctuation in the strains along the length is due to the noise and accuracy of the data logger 5.5.

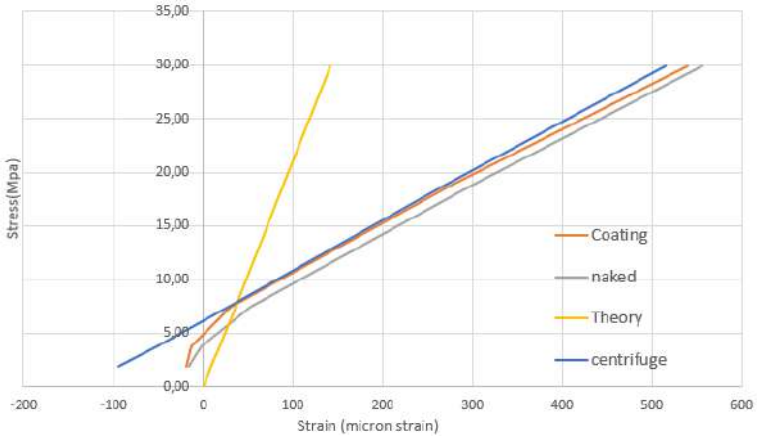

Figure 5.4: Strains measured theoretically, with Fiber, and centrifuge

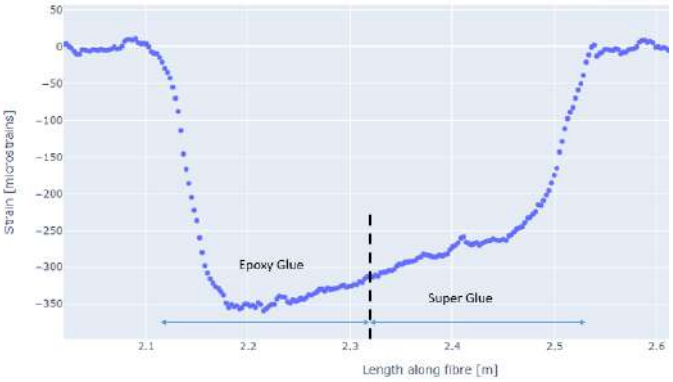

Figure 5.5: Strain readings throughout length of pile

5.3. Conclusions

To conclude, the objective of this report was to validate the results obtained while statically loading a pile. A reinforced concrete pile has been designed of dimensions $20 * 15 * 50cm$ which is embedded by the FO cables inside and strain gauge in the center of the pile but outside. Applying static load of up to 50kg, on top of the pile head in the incremental order of 5 kg. Through step by step loading of the pile, data was collected accordingly with the help of fTB 2505 datalogger and strain gauges. The data for concrete pile clearly indicates that there is relatively less difference observed between theoretical and gauge values as compared to datalogger strains. Certainly, it is hard to identify the exact location of the embedded fiber inside the concrete which make analysis of strains obtained through BOFDA technology and point based gauges really challenging. Also many uncertainties can occur while calculating strains with gauges due to improper bonding with the concrete, cracks below the gluing area, signal processing, data acquisition, and management. And also the accuracy specified on the technical document of the datalogger also is questionable.

Similar analysis conducted on the hollow steel pile of dimension 45*30cm with thickness of 0.3cm. But in steel pile 2 fibers are glued next to each other one is naked (without coating) and other with coating. Also for upper half length epoxy and lower half super glue is used to stick the fibers outside the surface of steel pile next to each other. Loading steel through jacking within the elastic limit causes no harm to the fibers. Both (naked and non naked) fibers give similar strain readings under the accuracy of the datalogger. Epoxy and super glue bonded really well with the steel pile and no slip was observed.

For future research loading needs to be applied on the pile till ultimate limit of the material. And then phenomenon like slippage, effect of coating can be looked upon into more depth while cracking occurs underneath the FO cable.

References

[1] J.-L. Briaud and L. Tucker. Piles in sand: a method including residual stresses. Journal of Geotechnical Engineering, 110(11):1666–1680, 1984.

[2] R. M. Buckley, R. A. McAdam, B. W. Byrne, J. P. Doherty, R. J. Jardine, S. Kontoe, and M. F. Randolph. Optimization of impact pile driving using optical fiber bragg-grating measurements. Journal of Geotechnical and Geoenvironmental Engineering, 146:04020082, 9 2020.

[3] K. Cápová, L. Velebil, and J. Velák. Laboratory and in-situ testing of integrated fbg sensors for shm for concrete and timber structures. Sensors (Switzerland), 20, 3 2020.

[4] N. de Battista, C. Kechavarzi, and K. Soga. Distributed fiber optic sensors for monitoring reinforced concrete piles using brillouin scattering. volume 9916, page 99160U. SPIE, 5 2016.

[5] P. Doherty, D. Igoe, G. Murphy, K. Gavin, J. Preston, C. McAvoy, B. W. Byrne, R. McAdam, H. J. Burd, G. T. Houlsby, C. M. Martin, L. Zdravkovi, D. M. Taborda, D. M. Potts, R. J. Jardine, M. Sideri, F. C. Schroeder, A. M. Wood, D. Kallehave, and J. S. Gretlund. Field validation of fibre bragg grating sensors for measuring strain on driven steel piles. Geotechnique Letters, 5:74–79, 2 2015.

[6] fibris Terre Systems GmbH. Distributed fiber-optic Brillouin sensing The fTB 2505 series Technical documentation, 8 2015.

[7] K. N. Flynn and B. A. McCabe. Instrumented concrete pile tests-part 2: Strain interpretation. Proceedings of the Institution of Civil Engineers: Geotechnical Engineering, 175:112–135, 2 2022.

[8] N. A. Hoult, O. Ekim, and R. Regier. Damage/deterioration detection for steel structures using distributed fiber optic strain sensors. Journal of Engineering Mechanics, 140:04014097, 12 2014.

[9] D. ir. Mandy Korff. Reader deep excavations design, execution and monitoring of deep excavations with retaining walls, 2018.

[10] H. Iwaki, H. Yamakawa, and A. Mita. Health monitoring system using fiber bragg grating -based sensors for a 12-story building with column dampers, 2001.

[11] M. Kamaya, Y. Kitsunai, and M. Koshiishi. True stress-strain curve acquisition for irradiated stainless steel including the range exceeding necking strain. Journal of Nuclear Materials, 465:316–325, 6 2015.

[12] C. Kechavarzi, L. Pelecanos, N. D. Battista, and K. Soga. Distributed fibre optic sensing for monitoring reinforced concrete piles. Geotechnical Engineering Journal of the SEAGS AGSSEA, 50, 2019.

[13] G. Kister, D. Winter, Y. M. Gebremichael, J. Leighton, R. A. Badcock, P. D. Tester, S. Krishnamurthy, W. J. Boyle, K. T. Grattan, and G. F. Fernando. Methodology and integrity monitoring of foundation concrete piles using bragg grating optical fibre sensors. Engineering Structures, 29:2048–2055, 9 2007.

[14] A. Klar, P. J. Bennett, K. Soga, R. J. Mair, P. Tester, R. Fernie, H. D. St John, and G. Torp-Peterson. Distributed strain measurement for pile foundations. Proceedings of the Institution of Civil Engineers-Geotechnical Engineering, 159(3):135–144, 2006.

[15] LUNA. ODiSI 6000 Series Optical Distributed Sensor Interrogators, 3 2022.

[16] J. G. MacGregor, J. K. Wight, S. Teng, and P. Irawan. Reinforced concrete: Mechanics and design, volume 3. Prentice Hall Upper Saddle River, NJ, 1997.

[17] A. Minardo, R. Bernini, and L. Zeni. A simple technique for reducing pump depletion in long-range distributed brillouin fiber sensors. IEEE Sensors Journal, 9:633–634, 6 2009.

[18] H. Mohamad, K. Soga, A. Pellew, and P. J. Bennett. Performance monitoring of a secant-piled wall using distributed fiber optic strain sensing. Journal of Geotechnical and Geoenvironmental Engineering, 137:1236–1243, 12 2011.

[19] W. Montero, R. Farag, V. Díaz, M. Ramirez, and B. L. Boada. Uncertainties associated with strain-measuring systems using resistance strain gauges. Journal of Strain Analysis for Engineering Design, 46:1–13, 1 2011.

[20] R. Nie, W. Leng, Q. Yang, and Y. F. Chen. Effects of pile residual loads on skin friction and toe resistance. Soil Mechanics and Foundation Engineering, 55:76–81, 5 2018.

[21] N. Nöther and M. Krcmar. Industry challenges on resolution, linearity and optical budget of high-accuracy distributed brillouin sensing. In Transforming the Future of Infrastructure through Smarter Information: Proceedings of the International Conference on Smart Infrastructure and ConstructionConstruction, 27–29 June 2016, pages 111–116. ICE Publishing, 2016.

[22] H. G. Poulos. Analysis of residual stress effects in piles. Journal of geotechnical engineering, 113(3):216–229, 1987.

[23] R. D. Rieke and J. C. Crowser. Interpretation of pile load test considering residual stresses. Journal of geotechnical engineering, 113(4):320–334, 1987.

[24] Seaway Heavy Lifting Engineering B.V. Pile Driveability and Installation Seaway Heavy Lifting Engineering B.V, 5 2009.

[25] W. Shen, X. Wang, L. Xu, and Y. Zhao. Strain transferring mechanism analysis of the substrate-bonded fbg sensor. Optik, 154:441–452, 2 2018.

[26] A. M. Van Der Veen and M. G. Cox. Error analysis in the evaluation of measurement uncertainty. Metrologia, 40(2):42, 2003.

[27] S. Watson, F. Zahn, and R. Park. Confining reinforcement for concrete columns. Journal of Structural Engineering, 120(6):1798–1824, 1994.

[28] Q. Zhang and Z. Xiong. Crack detection of reinforced concrete structures based on bofda and fbg sensors. Shock and Vibration, 2018, 2018.

[29] X. Zheng, B. Shi, H. H. Zhu, C. C. Zhang, X. Wang, and M. Y. Sun. Performance monitoring of offshore phc pipe pile using bofda based distributed fiber optic sensing system. Geomechanics and Engineering, 24:337–348, 2021.

[30] F. Zhu, P. Bai, J. Zhang, D. Lei, and X. He. Measurement of true stress-strain curves and evolution of plastic zone of low carbon steel under uniaxial tension using digital image correlation. Optics and Lasers in Engineering, 65:81–88, 2 2015.

6

Appendix

6.0.1. Eccentricity:

Eccentric Load refers to a load which is not acting through the line of the axis of the pile. The eccentric load can cause the pile to bend towards the eccentricity of the loading and hence generates a bending moment in the pile. The minimum eccentricity in pile should be 75mm.

1. 20mm.
2. H/30=500/30=16.66mm
   So eccentricity would be 20mm, which means distance from the center axis required should be 20mm on both axis. In the calculation, the size of the pile is taken as 20*15cm which is greater than 2cm in X as well as Y axis.

Long/ short column:

Length/ Height >12 is a long column whereas less than 12 is a short column.

$$500/150 = 3.34 = \text{Short column} \tag{6.1}$$

Figure 6.1: Cracks developed on concrete surface after curing

Figure 6.2: Cracks developed on concrete after curing